Author(s): Pasqualato, G.; Gottardo, A.; Mengoni, D.; Goasduff, A.; Valiente-Dobón, J. J.; Nowacki, F.; Péru, S.; Pillet, N.; de Angelis, G.; Bakes, S. D.; Bayram, T.; Bazzacco, D.; Benzoni, G.; Brugnara, D.; Cicerchia, M.; Colovic, P.; Cortés, M. L.; Gadea, A.; Galtarossa, F.; Górska, M.; Gozzelino, A.; Gregor, E.; Hubbard, N.; Illana, A.; Jurado, M.; Lenzi, S. M.; Mantovani, G.; Marchi, T.; Menegazzo, R.; Montaner-

Title: An alternative viewpoint on the nuclear structure towards 100Sn : Lifetime measurements in 105Sn

Please cite the original version:

Pasqualato, G., Gottardo, A., Mengoni, D., Goasduff, A., Valiente-Dobón, J.J., Nowacki, F., Péru, S., Pillet, N., de Angelis, G., Bakes, S. D., Bayram, T., Bazzacco, D., Benzoni, G., Brugnara, D., Cicerchia, M., Colovic, P., Cortés, M. L., Gadea, A., Galtarossa, F., . . . Zanon, I. (2023). An alternative viewpoint on the nuclear structure towards 100Sn : Lifetime measurements in 105Sn. Physics Letters B, 845, Article 138148. https://doi.org/10.1016/j.physletb.2023.138148
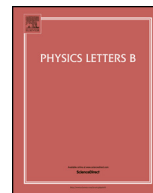
An alternative viewpoint on the nuclear structure towards ^{100}Sn: Lifetime measurements in ^{105}Sn

G. Pasqualato [a,b,c,*], A. Gottardo [d], D. Mengoni [a,b], A. Goasduff [a,b,d], J.J. Valiente-Dobón [d], F. Nowacki [e], S. Péru [f,g], N. Pillet [f,g], G. de Angelis [d], S.D. Bakes [d,h], T. Bayram [d,i], D. Bazzacco [d], G. Benzoni [j], D. Brugnara [b,d], M. Cicerchia [b,d], P. Colovic [k], M.L. Cortés [d,l], A. Gadea [m], F. Galtarossa [d], M. Górska [n], A. Gozzelino [d], E. Gregor [d], N. Hubbard [n,l], A. Illana [d,o], M. Jurado [m], S.M. Lenzi [a,b], G. Mantovani [d,b], T. Marchi [d], R. Menegazzo [a], A. Montaner-Pizá [a,b], D.R. Napoli [d], F. Recchia [a,b], M. Siciliano [p,q], D. Testov [a,b,r], S. Szilner [k], I. Zanon [d,s]

[a] INFN, Sezione di Padova, Padova, Italy
[b] Dipartimento di Fisica e Astronomia, Università di Padova, Padova, Italy
[c] IJCLab, IN2P3/CNRS, Université Paris-Saclay, Orsay, France
[d] INFN, Laboratori Nazionali di Legnaro, Legnaro, Italy
[e] IPHC, CNRS/IN2P3, Université de Strasbourg, Strasbourg, France
[f] CEA, DAM, DIF, Arpajon, France
[g] CEA, LMCE, Université Paris-Saclay, Bruyères-le-Châtel, France
[h] Department of Physics, University of Surrey, Guildford, UK
[i] Department of Physics, Karadeniz Technical University, Trabzon, Turkey
[j] INFN, Sezione di Milano, Milano, Italy
[k] Ruđer Bošković Institute, Zagreb, Croatia
[l] Institute for Nuclear Physics, Dept. of Physics, TU Darmstadt, Germany
[m] IFIC, CSIC-Universidad de Valencia, Valencia, Spain
[n] GSI Helmholtzzentrum für Schwerionenforschung GmbH - Darmstadt, Germany
[o] Accelerator Laboratory, Department of Physics, University of Jÿvaskylä, Jÿvaskylä, Finland
[p] DPhN/Irfu/CEA, Université de Paris-Saclay, Gif-sur-Yvette, France
[q] Physics Division, Argonne National Laboratory, Argonne (IL), United States
[r] Extreme Light Infrastructure - Nuclear Physics, IFIN-HH, Bucharest-Magurele, Romania
[s] Dipartimento di Fisica e Scienze della Terra, Università di Ferrara, Ferrara, Italy

ARTICLE INFO

ABSTRACT

This work aims at presenting an alternative approach to the long standing problem of the B(E2) values in Sn isotopes in the vicinity of the N=Z double-magic nucleus ^{100}Sn, until now predominantly measured with relativistic and intermediate-energy Coulomb excitation reactions. The direct measurement of the lifetime of low-lying excited states in odd-even Sn isotopes provides a new and precise guidance for the theoretical description of the nuclear structure in this region. Lifetime measurements have been performed in ^{105}Sn for the first time with the coincidence Recoil Distance Doppler Shift technique. The lifetime results for the $7/2^+_1$ first excited state and the $11/2^+_1$ state, $2^+(^{104}$Sn$) \otimes \nu 1g_{7/2}$ multiplet member, are discussed in comparison with state-of-the-art shell model and mean field calculations, highlighting the crucial contribution of proton excitation across the core of ^{100}Sn. The reduced transition probability B(E2) of the $11/2^+_1$ core-coupled state points out an enhanced staggering with respect to the B(E2; $2^+_1 \rightarrow 0^+_1$) in the even-mass ^{104}Sn and ^{106}Sn isotopes.

1. Introduction

The appearance of a shell structure is a common feature of confined many-body quantum systems. The atomic nucleus occupies

a special place among these systems, due to the emergence of a shell structure from the complex nucleon-nucleon interaction and to the possibility of studying shell closures far from stability. The study of shell evolution along semi-magic isotopic chains is key to understanding the extent to which conventional shell closures persist in exotic nuclei [1,2]. The N=Z=50 ^{100}Sn isotope is predicted to be the heaviest N=Z doubly magic nucleus, and hence many efforts have been devoted to understanding its structure by measuring neutron-deficient Sn isotopes, since its in-beam γ-ray spectroscopy is presently out of experimental reach [3]. In the even-mass nuclei $^{104-112}$Sn, the reduced transition strengths B(E2) from the first excited 2^+ state to the ground state are a probe of the N=Z=50 core robustness. B(E2) values deduced from Coulomb excitation experiments [4–13] do not follow the expected decreasing trend towards ^{100}Sn [14,15]. From the first large-scale shell-model studies for the Sn isotopes [4], it was evident that a pure generalized seniority scheme, with only neutron excitations in the valence space N=50-82 and a ^{100}Sn core, largely underestimates the experimental B(E2) values. To describe the experimental values, the inclusion of proton particle-hole excitations across the closed core of ^{100}Sn was required, as demonstrated also by later theoretical approaches [16,17]. This conclusion, together with larger than expected experimental B(E2) values observed in the neutron-deficient even-mass Sn isotopes [5,7,10–12,18–22], has spurred debate on the robustness of the Z=50 shell closure, otherwise supported by the β-decay studies in ^{100}Sn [23,24]. However, this question is far from being settled because of the large uncertainties in the experimental results in ^{104}Sn and ^{106}Sn, obtained via Coulomb excitation using radioactive ion beams [5,7,10–12]. For ^{104}Sn the three measured values are spread over a range compatible either with an increased collectivity [11,12] or a normal, seniority like decrease of the B(E2) values towards ^{100}Sn [10]. In this context, measurements with different methods and higher precision and accuracy in this region are crucial to guide the theoretical interpretations and help solving this long-standing puzzle.

The alternative approach to obtain the B(E2) strengths is via direct lifetime measurements of the 2_1^+ state. This technique is not affected by the same systematic uncertainty of relativistic Coulomb excitation experiments and can be used in fusion-evaporation reactions, where ^{104}Sn and ^{106}Sn are produced by using stable targets and intense stable beams. However, the presence of the long-lived 6_1^+ seniority isomer, feeding the lower-lying states, prevents a direct 2_1^+ lifetime measurement. Recently, lifetime measurements of the 2_1^+ and the 4_1^+ excited states in ^{106}Sn and ^{108}Sn were successfully performed via a multi-nucleon transfer reaction for the very first time [22]. The direct feeding of the excited states of interest in ^{106}Sn, allowed the lifetime measurement of the 2_1^+ state, albeit with a large error due to the small reaction cross section. In order to investigate E2 strengths in Sn isotopes lighter than ^{106}Sn with fusion-evaporation reactions, circumventing the presence of seniority isomers, we performed lifetime measurements in the odd-even ^{105}Sn nucleus. A simple understanding of the low-lying structure of semi-magic odd-even systems derives from the coupling of the unpaired neutron with the states of the neighbor even-even isotope [25]. This is evident from the structure of the ^{105}Sn level scheme which exhibits two well-defined bands (see Fig. 1) as a result of the coupling between the unpaired neutron in the $1g_{7/2}$ or in the $1d_{5/2}$ orbital with the ^{104}Sn core. The presence of two similar configurations characterizing the level scheme of light odd-mass Sn isotopes is justified by the small energy gap between the two neutron single-particle states $1g_{7/2}$ and $1d_{5/2}$ outside the ^{100}Sn core. Only two long lifetimes are reported for ^{105}Sn: the low-lying $7/2_1^+$ state at 200 keV excitation energy, with a lifetime $\tau = 480(120)$ ps, and the $17/2_1^+$ state at 2204 keV excitation energy, with $\tau = 550(70)$ ps [26,27]. This second state belongs to the band built on the $1d_{5/2}$ orbital, and does not significantly feed the
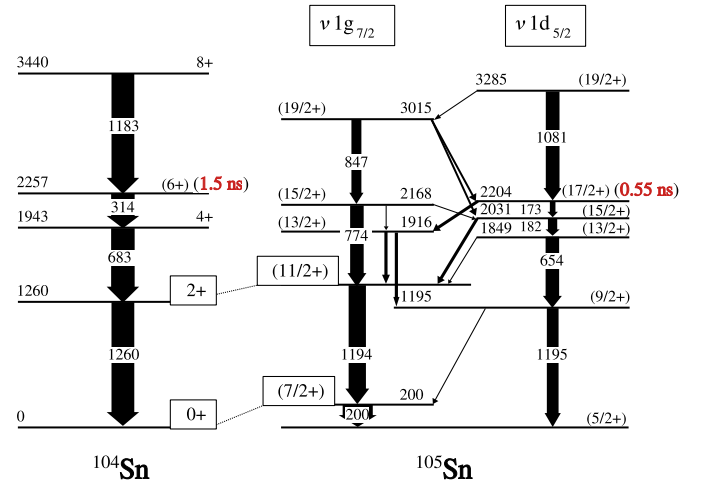

Fig. 1. Comparison between low-energy excited states in ^{104}Sn [28] and ^{105}Sn [29]. The width of the arrows represents the relative intensities. The two structures in ^{105}Sn, built on the $5/2_1^+$ ground state and the $7/2_1^+$ first excited state, are highlighted. The known lifetimes of the 6_1^+ seniority isomer in ^{104}Sn [28] and the $17/2_1^+$ isomer in ^{105}Sn [26] are reported and the coupling of the $7/2_1^+$ and $11/2_1^+$ states in ^{105}Sn with the 0_1^+ and 2_1^+ states in ^{104}Sn, respectively, are emphasized with dotted lines.

band on the $1g_{7/2}$ orbital. Therefore, the direct lifetime measurement of the ^{105}Sn $11/2_1^+$ state, namely coming for the coupling of the ^{104}Sn 2_1^+ state and the unpaired neutron in the $1g_{7/2}$ shell, is feasible. It provides the opportunity for a model-independent estimate of the B(E2) values in the neutron deficient Sn nuclei.

This work reports the first result for an E2 transition strength between low-lying excited states via lifetime measurements in ^{105}Sn, the most neutron-deficient Sn isotope in which the lifetime of states coupled to the 2^+ level of the even-even isotopes have been measured so far. Lifetime measurements after fusion-evaporation reactions provide a key tool to obtain model-independent electromagnetic strengths in odd-mass neutron-deficient Sn isotopes. The present contribution highlights how this approach can help to shed light on the nuclear structure in this region.

2. Experiment and results

The experiment was performed at the INFN Legnaro National Laboratories (Italy). The excited states in ^{105}Sn were populated via a fusion-evaporation reaction, using a 180-MeV ^{50}Cr beam delivered by the XTU-Tandem accelerator [30] and a ^{58}Ni target of 1-mg/cm^2 thickness, by the evaporation of two protons and one neutron from the compound nucleus ^{108}Te. The detection setup consisted of the GALILEO γ-ray spectrometer [31] coupled to the EUCLIDES Si-array [32], in order to enhance the reaction channel of interest among all the possible evaporation residues. GALILEO was composed of 25 Compton-suppressed HPGe detectors arranged in five rings at different angles with respect to the beam direction (152°, 129°, 119°, 61° and 51°). In this experiment EUCLIDES was placed only at forward angles [33] to enable the installation of the plunger device [34] inside the reaction chamber and perform lifetime measurements using the Recoil Distance Doppler Shift (RDDS) technique [35]. The stopper mounted on the plunger was a 16-mg/cm^2 layer of ^{197}Au. The reaction channel 2p1n was selected by applying the coincidence with at least one proton in EUCLIDES, in order not to excessively suppress the statistics. Data was collected for 12 target-to-stopper distances ranging from 10 μm to 8000 μm in order to guarantee sensitivity to lifetimes of few picoseconds as well as of hundreds picoseconds. Lifetimes in ^{105}Sn were measured in γ-γ coincidence by applying the Differential Decay Curve
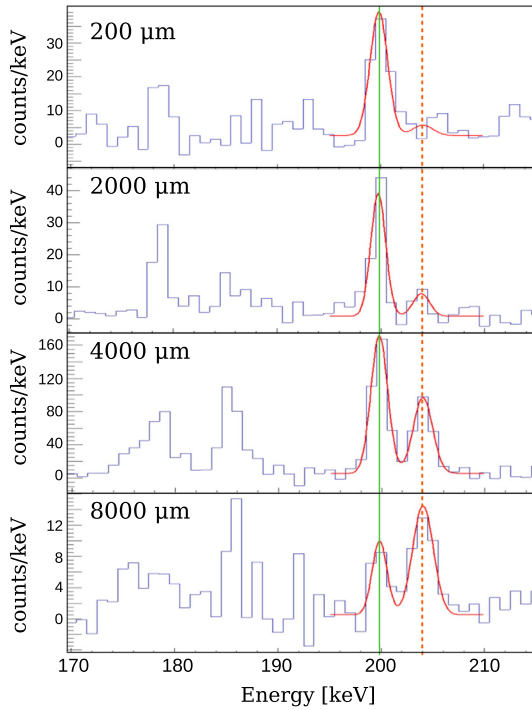
Fig. 2. Background-subtracted γ-ray spectra showing the shifted and the stopped components of the 200-keV, $7/2^+_1 \rightarrow 5/2^+_1$ transition of ^{105}Sn recorded with GALILEO detectors at 51° at different target-to-stopper distances. The stopped and the shifted components of the $7/2^+_1 \rightarrow 5/2^+_1$ transition are highlighted with a green continuous line and a red dashed line, respectively.

Method (DDCM) [36,37]. RDDS measurements in γ-γ coincidence are specifically advantageous when the nucleus is populated at high excitation energy, as in fusion-evaporation reactions, since it ensures a complete control of the feeding contribution. Moreover, the γ-γ coincidence is crucial in the analysis of the $11/2^+_1$-state lifetime since ^{105}Sn presents γ-ray transitions with similar energy in the two bands (see Fig. 1).

The velocity β of the recoiling nucleus ($\beta = 0.035(2)$ for ^{105}Sn) is measured from the energy of the γ-ray Doppler shifted components as a function of the angle of emission. The stopped and in-flight intensities are normalized to the total number of γ rays collected after the particle gate within the acquisition time of a single plunger distance. The experimental technique was validated by measuring known lifetimes in ^{105}In, which corresponds to the 3p-reaction channel, by using a γ-γ-2p coincidence condition to produce γ-ray spectra [38,39]. For ^{105}Sn, lifetimes are measured in γ-γ-1p coincidence (by gating on the in-flight component of the direct feeding transition) and the results are the following: $\tau(7/2^+_1)$ = 0.61(3) ns, $\tau(11/2^+_1)$ = 7(2) ps. The lifetime of the $7/2^+_1$ state measured in this experiment, for the first time in γ-γ coincidence, agrees within the error bars with the previous measurement $\tau = 480(120)$ ps [26] and significantly improves the precision. The projected spectra for the $7/2^+_1 \rightarrow 5/2^+_1$ transition are presented in Fig. 2, showing the evolution of the in-flight component with respect to the stopped one.

The analysis of the lifetime of the $11/2^+$ state requires merging the statistics collected from all 5 GALILEO rings after the gate on the in-flight component of the direct feeding transition. The stopped and shifted components suffer in fact from a reduction of statistics in the region of sensitivity due to the presence of the higher-lying longer-living state $27/2^+_1$ in the feeding pattern of the $11/2^+_1$ excited state. Fig. 3 shows separately the projected spectra including the sum of the stopped, not Doppler corrected, components and the sum of the shifted components, which are

Doppler corrected in order to merge the statistics from all different GALILEO rings at the nominal energy 1194 keV. The coincidence intensities are measured from the projected spectra by using a gaussian fit where the parameters sigma and centroid are constrained to vary in an optimized energy range. Fig. 4 presents the DDCM analysis for both the $7/2^+_1 \rightarrow 5/2^+_1$ and $11/2^+_1 \rightarrow 7/2^+_1$ transitions, performed with the Napatau software [40].

3. Discussion

From the measured lifetimes, transition probabilities can be calculated if the mixing ratio between the most probable multipolarity characterizing the transition is known. For the $7/2^+_1 \rightarrow 5/2^+_1$ transition, the experimental mixing ratio between the dominant multipolarities M1 and E2 is not known. Given the small energy of this excitation (200 keV), even a E2 mixing of $\sim 10\%$ would imply a B(E2) larger than 450 e^2fm^4 (15 Wu), which is an unrealistic value for such low-lying state in a semi-magic nucleus. Therefore, the character of the transition is assumed to be M1, with a strength of B(M1; $7/2^+_1 \rightarrow 5/2^+_1$) = 0.0107(6) μ^2_N. The $11/2^+_1 \rightarrow 7/2^+_1$ transition is a stretched E2 and the obtained value is B(E2; $11/2^+_1 \rightarrow 7/2^+_1$) = 50(15) e^2fm^4.

Different theoretical approaches are considered in order to interpret the obtained values. In the first place, a large scale shell-model calculations (LSSM) within the full sdg major shell ($g_{9/2}$, $g_{7/2}$, $d_{5/2}$, $d_{3/2}$, $s_{1/2}$) for both protons and neutrons. The calculations were performed up to $7p$-$7h$ excitations from the Z=N=50 core to ensure convergence, corresponding to a dimensionality of $60 \cdot 10^9$ basis states. The effective interaction is the one from the recent work of Ref. [22]. Different set of effective operators are used to assess the sensitivity of the present calculations to effects outside the model space: electric transitions are computed with three sets of effective charges (e_p, e_n). The standard (1.5e, 0.5e) values, the isovector values (1.35e, 0.65e), used in Ref. [22], and the recent values (1.11e, 0.84e) extracted in the vicinity of ^{100}Sn [41]. For gyromagnetic factors, either "bare" values or "effective" values are implemented, the latter usually used in $0\hbar\omega$ calculations, with a quenching factor 0.75 of the spin g factors and orbital g factors equal to 1.1 for protons and -0.1 for neutrons [42–44]. In a second approach, the Multiparticle-Multihole (MPMH) configuration mixing model [45–47] is used to investigate B(M1) transitions by using the D1M Gogny interaction [48]. Calculations are performed by considering different neutron valence spaces, with and without proton excitations from the $1g_{9/2}$ to the $1g_{7/2}$ and $2d_{5/2}$ orbitals. This analysis allows one to identify the contribution of p-h excitations in different frameworks and indicates as an optimal choice the full sdg valence space for neutrons and the $1g_{9/2}$, $1g_{7/2}$, $2d_{5/2}$ valence space for protons. Bare operators are used and only results for M1 transition strengths are presented. Finally, a consistent approach including Gogny force and the quasi-random phase approximation (QRPA) [49] is used to calculate the $9/2^+_1$ and $11/2^+_1$ excited states, as phonons built with coherent states of two quasi-particle excitations on Hartree-Fock-Bogoliubov (HFB) solutions obtained by blocking the $5/2^+$ and $7/2^+$ orbitals, respectively. This blocking assumption enables the calculations of the B(E2; $11/2^+_1 \rightarrow 7/2^+_1$) and its validity is supported by MPMH calculations performed with the same D1M Gogny interaction. MPMH calculations show in fact the similarity between the wave functions of the $9/2^+_1$ state and the $5/2^+_1$ ground state and between the $11/2^+_1$ and the $7/2^+_1$ excited states, thus supporting the assumption of independent QRPA calculations on top of HFB solution with blocking on the $d_{5/2}$ K=5/2 state or the $g_{7/2}$ K=7/2 state. The present HFB+QRPA calculations, applied to an odd-mass nucleus, are similar of those performed in Ref. [50] and supplement previous studies on even-mass Sn isotopes [49,51].
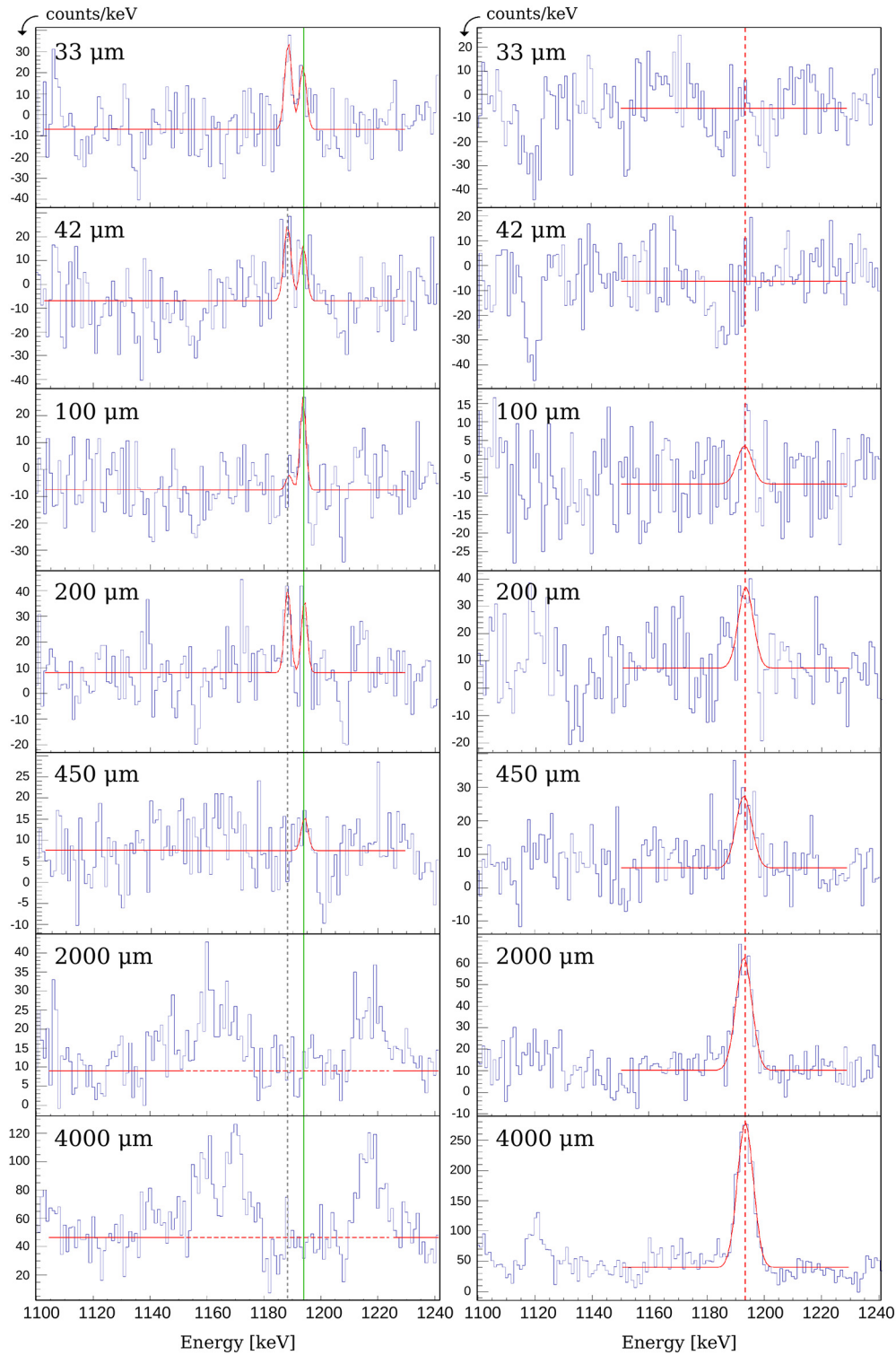
Fig. 3. Background-subtracted γ-ray spectra showing the $11/2^+_1 \rightarrow 7/2^+_1$ transition in coincidence with the $15/2^+_1 \rightarrow 11/2^+_1$ feeding transition. Only the six most relevant target-to-stopper distances are shown. The left-side panels show the sum of no-Doppler corrected spectra from all GALILEO rings. The stopped component, highlighted with a green continuous line, is fitted together with a contaminant, marked in the figure with a dotted gray line. The right-side panels show the sum of the spectra from all GALILEO rings after Doppler correction. The in-flight component is highlighted with a red dashed line.

The double-band character of the level scheme of ^{105}Sn, as presented in Fig. 1, can be interpreted as the coupling of the unpaired neutron in the $g_{7/2}$ or the $d_{5/2}$ orbital to the yrast states of ^{104}Sn. Both LSSM and MPMH calculations confirm this interpretation, showing the predominant occupation of the $g_{7/2}$ and $d_{5/2}$ neutron orbitals by the unpaired neutron in the bands built on the $7/2^+$ and $5/2^+$, respectively. The experimental transition probabil-

ities and the calculated ones are reported in Table 1. For the LSSM calculations, the presented value is the one with the (1.5e, 0.5e) standard effective charges, in better agreement with our result.

Concerning the $7/2^+_1 \rightarrow 5/2^+_1$ transition, if a single-particle nature is considered, i.e. a valence neutron passing from the $1g_{7/2}$ to the $2d_{5/2}$ orbital, it would then be an ℓ-forbidden M1. The non-zero value of the experimental B(M1) indicates that this transition
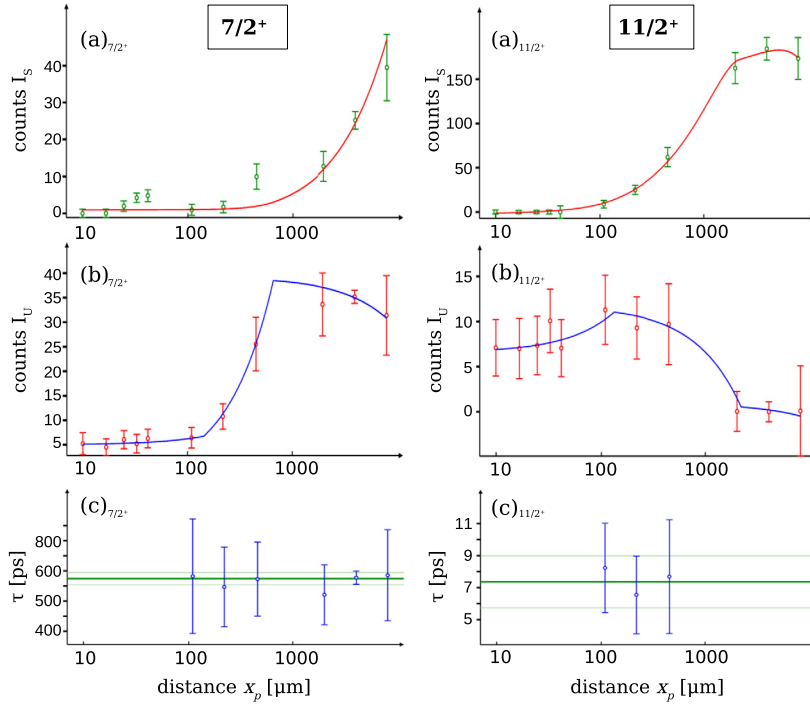
Fig. 4. DDCM analysis [37] of γ-γ coincidence data for the $7/2_1^+ \rightarrow 5/2_1^+$ (on the left panels) and $11/2_1^+ \rightarrow 7/2_1^+$ (on the right panels) transitions in ^{105}Sn. Data show the intensities measured with GALILEO detectors at 119° for the $7/2_1^+ \rightarrow 5/2_1^+$ transition and with all GALILEO detectors for the $11/2_1^+ \rightarrow 7/2_1^+$ transition. The error bars correspond to statistical errors. Each pair of panels reports: (a) normalized intensities of the shifted components I_S with the fitting function $f(x)$ corresponding to three smoothly connected polynomials of second order; (b) normalized intensities of the stopped components I_U with the fitting function proportional to the derivative of $f(x)$; (c) weighted average (thick green line) of the lifetimes $\tau(x_p)$ calculated at each plunger distance, with the associated uncertainties shown with thin green lines.

Table 1

Transition probabilities obtained from the lifetimes measured in the present experiment for the excited states $7/2_1^+$ and $11/2_1^+$ in ^{105}Sn. The experimental results are compared with LSSM$^{(1)}$ calculations using standard effective charge values (1.5e, 0.5e), QRPA and MPMH calculations.

	exp	LSSM$^{(1)}$	QRPA	MPMH
B(M1; $7/2^+ \rightarrow 5/2^+$) [μ_N^2]	0.0107(6)	0.0017		0.0037
B(E2; $11/2^+ \rightarrow 7/2^+$) [e^2fm^4]	50(15)	118	40	

is not of pure single-particle nature. LSSM and MPMH calculations also predict a non-zero value for this transition strength and the calculated wave functions show that in addition to multiple neutron excitations, the role of proton excitations from the ^{100}Sn core is crucial in the wave functions composition of the $5/2_1^+$ and $+7/2_1^+$ states in ^{105}Sn. In this regard, the measured B(M1; $7/2^+ \rightarrow 5/2^+$) in ^{105}Sn is a sensitive probe of the effectiveness of our models describing the breaking of the ^{100}Sn core. The LSSM value of 0.0017 μ_N^2 for the B(M1; $7/2^+ \rightarrow 5/2^+$) reported in Table 1 is obtained with effective values of the gyromagnetic factors. The same quantity calculated with bare values of the gyromagnetic factors works out at 0.0039 μ_N^2, in very good agreement with the value obtained by MPMH calculations with bare operators.

The E2 strength for the $11/2_1^+ \rightarrow 7/2_1^+$ transition shows a surprisingly small value if compared with the experimental B(E2; $2^+ \rightarrow 0^+$) obtained for ^{104}Sn (200(80) e^2fm^4 [10], 360(74) e^2fm^4 [11] and 346(56) e^2fm^4 [12]). The small ratio between the B(E2; $11/2_1^+ \rightarrow 7/2_1^+$) in ^{105}Sn and the average of the existing B(E2; $2^+ \rightarrow 0_1^+$) values for ^{104}Sn can be partially ascribed to a different seniority changing factor for the $11/2_1^+ \rightarrow 7/2_1^+$ transition (from $\nu = 3$ to $\nu = 1$) with respect to the $2_1^+ \rightarrow 0_1^+$ transitions (where seniority changes from $\nu = 2$ to $\nu = 0$). This yields to a reduction factor of about 0.8 in a case of single-j seniority where only the $g_{7/2}$ orbital is considered [52]. However, a generalized seniority
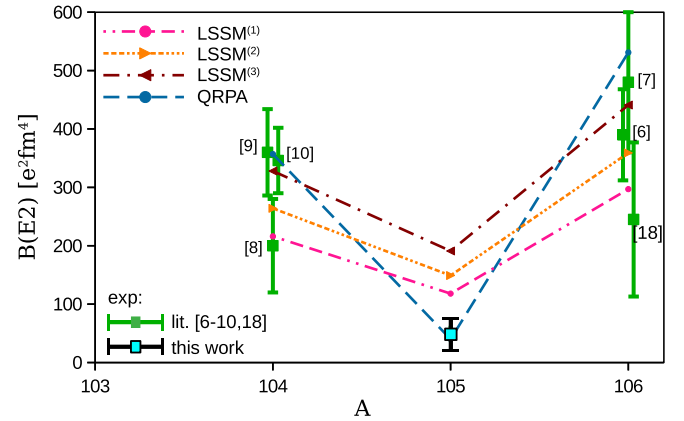
Fig. 5. Calculated B(E2) values for the $2^+ \rightarrow 0^+$ transition in ^{104,106}Sn and for the $11/2^+ \rightarrow 7/2^+$ transition in ^{105}Sn by QRPA, LSSM$^{(1)}$ with (1.50e, 0.50e) effective charges, LSSM$^{(2)}$ with (1.35e, 0.65e) effective charges and LSSM$^{(3)}$ with (1.11e, 0.84e) effective charges. See text for details. Experimental values are reported from this work for ^{105}Sn and for ^{104}Sn, ^{106}Sn from the works in Ref. [10–12,5,7,22].

approach for non-degenerate $d_{5/2}$ and $g_{7/2}$ orbitals can be more adequate [14]. This calculation [53] leads to a smaller factor of about 0.6, which is still not sufficient to account for the ratio between the experimental B(E2) values.

The trend of de-excitation transition probabilities from the 2_1^+ in the even-even neighboring isotopes and the $11/2_1^+$ coupled state in the odd-even Sn is shown in Fig. 5 for ^{104}Sn, ^{105}Sn and ^{106}Sn. The experimental values are compared with the three sets of LSSM calculations, using different effective charges, and QRPA calculations. One can notice that for these nuclei, the B(E2) staggering trend is qualitatively reproduced by both QRPA and LSSM calculations. Fig. 5 shows that, in view of the large uncertainties of the experimental B(E2; $2^+ \rightarrow 0^+$) in even-mass neighbors Sn iso-

topes, the direct lifetime measurements in odd-even nuclei can provide an effective anchor point for different theoretical models. From the comparison between LSSM calculations and the actual measurements in ^{104,106}Sn is not possible to discriminate between the different sets of effective charges, while the measurement of the $11/2^+ \rightarrow 7/2^+$ transition in ^{105}Sn suggests a preference for the "standard" effective charges (LSSM$^{(1)}$). This would imply a LSSM prediction in better agreement with the inferior values of the experimental B(E2) in the ^{104}Sn and ^{106}Sn isotopes, from Ref. [10] and Ref. [22] respectively. On the other hand, the QRPA approach, predicts large B(E2; $2^+ \rightarrow 0^+$) values for ^{104,106}Sn, in better agreement with the Coulex measurements of Ref. [11,12,7], while also being in excellent agreement with the present result. From the analysis of the wave functions of LSSM calculations for ^{104}Sn and ^{105}Sn one can notice that the percentage of proton excitations from the $1g_{9/2}$ shell for both the $7/2_1^+$ and the $11/2_1^+$ states is similar with respect to the 0_1^+ and 2_1^+ states in ^{104}Sn. The wave function obtained from the QRPA calculations for the $11/2_1^+$ state in ^{105}Sn has also a proton composition similar to the one of the 2^+ states in neighboring even isotopes, but it involves less proton p-h excitations across Z=50, suggesting that in this calculation a difference of few percentage of proton contribution in the wave function results in a larger difference on the calculated B(E2) values.

The precision of the experimental measurement obtained in this work is crucial to constrain the different theoretical predictions. While both LSSM and QRPA calculations predict the observed odd-even staggering, the value which comes closer to our result is provided by the QRPA approach, which uses a different Hamiltonian based on the Gogny force and a larger valence space for both protons and neutrons.

4. Conclusion

In conclusion, the lifetime of the $11/2_1^+$ and the $7/2_1^+$ excited states in ^{105}Sn were measured for the first time with the Recoil Distance Doppler Shift technique in γ-γ coincidence via the ^{58}Ni(^{50}Cr, $2p1n$)^{105}Sn fusion-evaporation reaction. The comparison of the experimental transition probabilities with both LSSM and beyond mean-field models provided an insight on the role of proton and neutron p-h excitations across the N=Z=50 shell closure. In particular, the small ^{105}Sn B(E2; $11/2^+ \rightarrow 7/2^+$)=50(15) e^2fm^4 value obtained in this work is at variance with the large difference with respect to the E2 strengths of the 2_1^+ state in even-mass neutron-deficient Sn isotopes observed in all existing measurements. QRPA and LSSM calculations correctly predict an enhanced reduction of the B(E2) in ^{105}Sn with respect to the expectations of the single-j seniority model. The smaller value calculated from QRPA is in finer accordance with our accurate experimental result. This work shows that precise lifetime measurements in odd-even neutron-deficient Sn isotopes are crucial in constraining the different models and shedding light on the long-standing problem of the B(E2) values towards ^{100}Sn. The present result calls in particular for a similar measurement in ^{103}Sn, ^{107}Sn and ^{109}Sn, which can be effectively produced in fusion-evaporation reactions [54], to better define an "odd-even" B(E2) trend in Sn isotopes from direct lifetime measurements.

Declaration of competing interest

The authors declare that they have no known competing financial interests or personal relationships that could have appeared to influence the work reported in this paper.

Data availability

Data will be made available on request.

Acknowledgements

References

[1] O. Sorlin, M.-G. Porquet, Prog. Part. Nucl. Phys. 61 (2008) 602–673.

[2] T. Otsuka, A. Gade, O. Sorlin, T. Suzuki, Y. Utsuno, Rev. Mod. Phys. 92 (2020) 015002.

[3] T. Faestermann, M. Górska, H. Grawe, Prog. Part. Nucl. Phys. 69 (2013).

[4] A. Banu, J. Gerl, C. Fahlander, M. Górska, H. Grawe, T.R. Saito, et al., Phys. Rev. C 72 (2005) 061305(R).

[5] C. Vaman, C. Andreoiu, D. Bazin, A. Becerril, B.A. Brown, C.M. Campbell, et al., Phys. Rev. Lett. 99 (2007) 162501.

[6] J. Cederkäll, A. Ekström, C. Fahlander, A.M. Hurst, M. Hjorth-Jensen, et al., Phys. Rev. Lett. 98 (2007) 172501.

[7] A. Ekström, J. Cederkäll, C. Fahlander, M. Hjorth-Jensen, F. Ames, P.A. Butler, et al., Phys. Rev. Lett. 101 (2008) 012502.

[8] D.D. DiJulio, J. Cederkäll, C. Fahlander, A. Ekström, M. Hjorth-Jensen, et al., Phys. Rev. C 86 (2012) 031302(R).

[9] D.D. DiJulio, J. Cederkäll, C. Fahlander, A. Ekström, M. Hjorth-Jensen, et al., Eur. Phys. J. A 48 (2012) 105.

[10] G. Guastalla, D.D. DiJulio, M. Górska, J. Cederkäll, P. Boutachkov, P. Golubev, S. Pietri, H. Grawe, F. Nowacki, K. Sieja, et al., Phys. Rev. Lett. 110 (2013) 172501.

[11] V.M. Bader, A. Gade, D. Weisshaar, B.A. Brown, T. Baugher, D. Bazin, et al., Phys. Rev. C 88 (2013) 051301(R).

[12] P. Doornenbal, S. Takeuchi, N. Aoi, M. Matsushita, A. Obertelli, D. Steppenbeck, et al., Phys. Rev. C 90 (2014) 061302(R).

[13] P.A. Butler, J. Cederkall, P. Reiter, J. Phys. G, Nucl. Part. Phys. 44 (2017) 044012.

[14] I. Talmi, Nucl. Phys. A 172 (1971) 1–24.

[15] J.J. Ressler, R.F. Casten, N.V. Zamfir, C.W. Beausang, R.B. Cakirli, H. Ai, et al., Phys. Rev. C 69 (2004) 034317.

[16] T. Togashi, Y. Tsunoda, T. Otsuka, N. Shimizu, M. Honma, Phys. Rev. Lett. 121 (2018) 062501.

[17] A.P. Zuker, Phys. Rev. C 103 (2021) 024322.

[18] J. Cederkäll, A. Ekström, C. Fahlander, A.M. Hurst, M. Hjorth-Jensen, F. Ames, et al., Phys. Rev. Lett. 98 (2007) 172501.

[19] P. Doornenbal, P. Reiter, H. Grawe, H.J. Wollersheim, P. Bednarczyk, L. Caceres, et al., Phys. Rev. C 78 (2008) 031303(R).

[20] R. Kumar, P. Doornenbal, A. Jhingan, R.K. Bhowmik, S. Muralithar, S. Appannababu, et al., Phys. Rev. C 81 (2010) 024306.

[21] T. Bäck, C. Qi, B. Cederwall, R. Liotta, F. Ghazi Moradi, A. Johnson, R. Wyss, R. Wadsworth, Phys. Rev. C 87 (2013) 031306(R).

[22] M. Siciliano, J.J. Valiente-Dobón, A. Goasduff, F. Nowacki, A.P. Zuker, D. Bazzacco, et al., Phys. Lett. B 806 (2019) 135474.

[23] C. Hinke, M. Böhmer, P. Boutachkov, T. Faestermann, H. Geissel, J. Gerl, et al., Nature 486 (2012) 341345.

[24] D. Lubos, J. Park, T. Faestermann, R. Gernhäuser, R. Krücken, M. Lewitowicz, et al., Phys. Rev. Lett. 122 (2019) 222502.

[25] A. De-Shalit, Phys. Rev. 122 (1961) 1530.

[26] T. Ishii, et al., Jaeri Tandem & V.D.G., Annual Report 1993, vol. 94-008, 1994, p. 11.

[27] M. Ogawa, H. Tsuchida, A. Makishima, T. Ishii, M. Ishii, G. Momoki, K. Ogawa, Phys. Scr. 1995 (1995) 289.

[28] M. Górska, H. Grawe, D. Kast, G. de Angelis, P.G. Bizzeti, B.A. Brown, et al., Phys. Rev. C 58 (1998) 108.

[29] A. Gadea, G. de Angelis, C. Fahlander, M. De Poli, E. Farnea, Y. Li, et al., Phys. Rev. C 55 (1997) R1.

[30] C. Signorini, Rev. Phys. Appl. (Paris) 12 (1977) 1361–1367.

[31] A. Goasduff, D. Mengoni, F. Recchia, J.J. Valiente-Dobon, et al., Nucl. Instrum. Methods Phys. Res., Sect. A 1015 (2021) 165753.

[32] D. Testov, D. Mengoni, A. Goasduff, et al., Eur. Phys. J. A 55 (2019).

[33] J. Bradbury, et al., Nucl. Instrum. Methods Phys. Res., Sect. A 979 (2020) 164345.

[34] C. Müller-Gatermann, F. von Spee, A. Goasduff, et al., Nucl. Instrum. Methods Phys. Res., Sect. A 920 (11) (2019) 95–99.

[35] T.K. Alexander, J.S. Forster, Adv. Nucl. Phys. (1978) 197–331.

[36] A. Dewald, et al., Z. Physik A - Atomic Nuclei 334 (1989) 163–175.

[37] A. Dewald, et al., Prog. Part. Nucl. Phys. 679 (2012) 786.

[38] G. Pasqualato, et al., LNL Annual Report 19, 46, 2020.

[39] G. Pasqualato, et al., Acta Phys. Pol. B 51 (2020) 823.

[40] B. Saha, Napatau or Tk-Lifetime-Analysis, unpublished.

[41] H. Grawe, K. Straub, T. Faestermann, M. Górska, C. Hinke, R. Krücken, F. Nowacki, et al., Phys. Lett. B 820 (2021) 136591.

[42] E. Caurier, G. Martínez-Pinedo, F. Nowacki, A. Poves, A.P. Zuker, Rev. Mod. Phys. 77 (2005) 427.

[43] E. Caurier, A. Poves, A.P. Zuker, Phys. Rev. Lett. 74 (1995) 1517.

[44] K. Langanke, G. Martínez-Pinedo, P. von Neumann-Cosel, A. Richter, Phys. Rev. Lett. 93 (2004) 202501.

[45] N. Pillet, J.F. Berger, E. Caurier, Phys. Rev. C 78 (2008) 024305.

[46] C. Robin, N. Pillet, D. Peña Arteaga, J.F. Berger, Phys. Rev. C 93 (2016) 024302.

[47] C. Robin, N. Pillet, M. Dupuis, J. Le Bloas, D. Peña Arteaga, J.F. Berger, Phys. Rev. C 95 (2017) 044315.

[48] S. Goriely, S. Hilaire, M. Girod, S. Péru, Phys. Rev. Lett. 102 (2009) 242501.

[49] S. Péru, M. Martini, Eur. Phys. J. A 50 (2014) 88.

[50] S. Goriely, S. Péru, G. Colò, X. Roca-Maza, I. Gheorghe, D. Filipescu, H. Utsunomiya, Phys. Rev. C 102 (2020) 064309.

[51] A. Corsi, et al., Phys. Lett. B 743 (2015) 451–455.

[52] A. de-Shalit, I. Talmi, Nuclear Shell Theory, Academic Press, NY, 1965.

[53] P. Van Isacker, private communication.

[54] C. Fahlander, M. Palacz, D. Rudolph, D. Sohler, J. Blomqvist, J. Kownacki, et al., Phys. Rev. C 63 (2001) 021307(R).